Hydrodynamic Characteristics and Gas–Liquid Mass Transfer in a Biofilm Airlift Suspension Reactor

C. Nicolella, M. C. M. van Loosdrecht, R. G. J. M. van der Lans, J. J. Heijnen

Kluyver Institute for Biotechnology, Delft University of Technology, Julianalaan 67, 2628 BC Delft, The Netherlands; telephone: 31-15-2781618; fax: 31-15-2782355; e-mail: c.nicolella@ic.ac.uk

Abstract: The hydrodynamics and mass transfer, specifically the effects of gas velocity and the presence and type of solids on the gas hold-up and volumetric mass transfer coefficient, were studied on a lab-scale airlift reactor with internal draft tube. Basalt particles and biofilm-coated particles were used as solid phase. Three distinct flow regimes were observed with increasing gas flow rate. The influence of the solid phase on the hydrodynamics was a peculiar characteristic of the regimes. The volumetric mass transfer coefficient was found to decrease with increasing solid loading and particle size. This could be predominantly related to the influence that the solid has on gas hold-up. The ratio between gas hold-up and volumetric mass transfer coefficient was found to be independent of solid loading, size, or density, and it was proven that the presence of solids in airlift reactors lowers the number of gas bubbles without changing their size. To evaluate scale effects, experimental results were compared with theoretical and empirical models proposed for similar systems. © 1998 John Wiley & Sons, Inc. *Biotechnol Bioeng* **60**: 627–635, 1998.

Keywords: airlift reactor; biofilm; hydrodynamics; mass transfer

INTRODUCTION

The determination of the gas and solids hold-ups and volumetric mass transfer coefficient is an important factor in the design and operation of airlift reactors and has been the subject of much research interest. Extensive data are available for the estimation of design parameters in two-phase systems (Chisti, 1989). However, only a few studies have dealt with the specific case of three-phase airlift reactors and there is still no universally applicable relation describing the influence of all types of particles in any weight fraction in any liquid and for any reactor scale (Beenackers and van Swaaij, 1993).

Most of the articles on the hydrodynamics and mass transfer of three-phase airlift reactors have dealt with systems of relatively small scale. The influence of the presence of solids has been reported for various types of particles including glass beads (Koide et al., 1985), plastic beads

(Miyahara and Kawate, 1993), polystyrene cylinders (Hwang and Lu, 1997), activated carbon particles (Muroyama et al., 1985) Raney nickel particles (Gavroy et al., 1995), and calcium-alginate beads (Lu et al., 1995). For the case of biofilm-coated particles, Ryhiner et al. (1986) reported that the gas–liquid volumetric mass transfer coefficient in a three-phase biofilm fluidized sand-bed reactor decreased (in the range 0.02 to 0.04 s^{-1}) with increasing amounts of clean sand and was almost independent of the sand fraction with biofilm-covered sand. No direct information is available on biofilm airlift suspension reactors in which the solid phase is comprised of biofilm-coated particles, although these systems found useful large-scale industrial applications in wastewater treatment processes (Heijnen et al., 1990). Therefore, it seems important to understand how the presence of biofilm covering the solid particles may affect hydrodynamics and mass transfer in three-phase airlift reactors.

Empirical (Koide et al., 1985) and theoretical (Livingston and Zhang, 1993) models have also been proposed to describe the hydrodynamics of small-scale systems (0.001 to 0.01 m^3). Only recently, Heijnen et al. (1997) proposed a model for the hydrodynamic behavior of large-scale three-phase airlift reactors (0.1 to 500 m^3).

This work presents the experimental characterization of hydrodynamics and mass transfer in a lab-scale three-phase airlift reactor with an internal draft tube. Both basalt particles and biofilm-coated particles were used as solid phase. The influence of solid loading, size, and density on gas hold-up and gas–liquid volumetric mass transfer coefficient was investigated with specific attention to the peculiarities under different flow regimes. The results of the investigation are compared with literature data using small- and full-scale systems to evaluate the effect of scale.

MATERIALS AND METHODS

A concentric-tube airlift reactor with a three-phase separator (working volume 1.5 L) was used throughout this study. The reactor has been described by Gjaltema et al. (1995), and the essential details are given in Figure 1. The temperature of the reactor was maintained at 24°C by means of a

---

Correspondence to: C. Nicolella
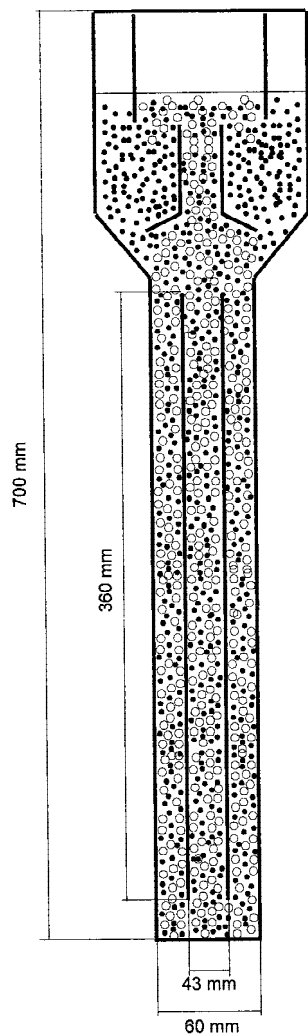
Figure 1. Experimental set-up.

thermostated water jacket. All experiments were performed at ambient pressure. The gas phase was sparged in the draught tube at the bottom of the reactor by means of a sintered glass sparger. The gas flow rate was controlled by means of a mass flow controller system. The superficial gas velocity, referred to the total column cross-section, ranged up to 150 mm/s. Tap water was the batch liquid used for all experiments.

Basalt particles (density 3010 kg/m³) and biofilm-coated particles were used as solid. Biofilm-coated particles were obtained from a biofilm airlift suspension reactor operated with municipal wastewater at Zandaam (NL). For both basalt particles and biofilm-coated particles, four size cuts of approximately uniform size were obtained by sieving. For each size fraction the particle average equivalent diameter was determined by means of a two-dimensional analysis system (Galai Cue 2, Betaversion 4.5, coupled with an Olympus SZH microscope); in the case of biofilm-coated particles, the average equivalent diameter of the bare carriers was also estimated through image analysis. The density of the biofilm was estimated by weighing the mass of dry

biomass of a known volume of biofilm-coated particles. The results of these measurements are reported in Table I. The terminal settling velocities in this table are calculated according to the relationship reported by Perry and Green (1984), assuming the particles were smooth spheres.

The influence of basalt loading was studied by using 0.34-mm basalt particles; the influence of biofilm loading was studied by using 1.95-mm particles; the solid concentration varied from 0 to 267 kg/m³ for basalt, and from 0 to 134 kg/m³ for biofilm-coated particles. The influence of particle size was studied at constant solid hold-up, $\varepsilon_S = 2.2\%$ for basalt, and $\varepsilon_S = 12\%$ for biofilm-coated particles. All data reported are for situations in which the solid was completely suspended in the reactor. The overall gas hold-up was determined by using the volume expansion technique (Chisti, 1987).

The volumetric mass transfer coefficient was determined by means of the transient gassing-in technique (Fuchs et al., 1971). All experiments were performed with batch liquid and solid phase and continuous gas flow. At the beginning of each experiment nitrogen was sparged to desorb the dissolved oxygen from the liquid and biofilm phase, then a preadjusted air flow was fed into the column by switching two three-way valves simultaneously. The increase in oxygen concentration in the liquid phase was measured by means of an oxygen probe (MTW-OXI 196) with response times of about 6 s and 15 s to reach 63% and 95% of a step change, respectively.

THEORY

Different oxygen balance equations were used for the case of basalt and biofilm-coated particles to estimate the gas–liquid volumetric mass transfer coefficient through a fitting procedure using probe response data.

Due to the low gas residence time in the column (estimated at less than 1.2 s for all experiments) the oxygen depletion in the gas phase, as well as the variation of $k_L a$ and oxygen concentration in the gas phase during the start-up of the dynamic method (when the gas phase is switched from nitrogen to oxygen), were neglected. Furthermore, complete mixing of the liquid phase was assumed. Under

Table I. Size, density and terminal settling velocity of particles used in the present experiments.

Type	Particle size (mm)	Support size (mm)	Particle density (kg/m³)	Settling velocity (mm/s)
Basalt	0.14	—	3010	19
	0.34	—	3010	52
	0.58	—	3010	96
	0.75	—	3010	129
Biofilm	0.47	0.29	1543	30
	0.91	0.45	1309	40
	1.67	0.52	1092	43
	1.95	0.64	1095	49

these assumptions, oxygen dynamics can be described through the simple models discussed in what follows.

Oxygen Balance in the Presence of Basalt Particles

In the case of basalt particles the oxygen balance in the liquid phase is:

$$V_L \frac{dC_L}{dt} = k_L A_G (C^* - C_L) \qquad (1)$$

Oxygen Balance in the Presence of Biofilm-Coated Particles

In the case of biofilm-coated particles, the adsorption in the biofilm must be taken into account. It was assumed that the oxygen diffusion in the biofilm is much faster than the liquid–solid transfer, so that the oxygen can be considered uniformly distributed within the biofilm. This assumption was verified by comparing the solution of the resulting simplified model with the solution of a more complete model describing the diffusion within the biofilm through Fick's law. The error in the $k_L a$ estimation made by using the simplified model was less than 4% for solid hold-up less than 12%. On the other hand, neglecting the oxygen adsorption in the biofilm [i.e., using Eq. (1)] in the estimation of $k_L a$ led to errors higher than 15% for solid hold-ups higher than 6%. The oxygen dynamics is therefore described in the following equations:

$$V_L \frac{dC_L}{dt} = k_L A_G (C^* - C_L) - k_S A_B (C_L - C_B) \qquad (2)$$

$$V_B \frac{dC_B}{dt} = k_S A_B (C_L - C_B) \qquad (3)$$

Sensitivity analysis of model equations to parameters showed that the model solution for the inherent initial conditions is insensitive to k_S, so that a rough estimation of this parameter should be sufficient to calculate a reliable value of $k_L a$. The correlation proposed by Sanger and Deckwer (1981) for aerated suspensions was used to estimate k_S.

For both basalt and biofilm-coated particles, V_L was calculated as:

$$V_L = V_R (1 - \varepsilon_S - \varepsilon_G) \qquad (4)$$

where ε_G and ε_S are gas and solid hold-up, respectively, and V_R is the total reactor volume. Henry's law was applied to calculate the liquid-side oxygen concentration at the gas–liquid interphase (C^*).

The effect of the probe response was taken into account by assuming a first-order model for the probe response:

$$\frac{dC_P}{dt} = k_P (C_L - C_P) \qquad (5)$$

The initial conditions inherent to the gassing-in technique are:

$$t = 0: C_P = C_L = C_B = 0 \qquad (6)$$

Model equations were fitted to the experimental probe response to obtain the volumetric mass transfer coefficient, here referring to the reactor volume

$$\left(k_L a = \frac{k_L A_G}{V_R} \right).$$

The nonlinear least-squares estimation tool of Aquasim (Reichert, 1994) was used to perform the calculations.

RESULTS AND DISCUSSION

Flow Regimes

It has been reported (Heijnen et al., 1997) that three flow regimes exist for three-phase airlift systems when gas velocity increases: (1) no gas entrainment in the downcomer; (2) gas entrainment, but no gas circulation; and (3) complete gas circulation. Regime 1 (no gas entrainment) was visually observed in the lab-scale reactor used in this study for gas superficial velocities of up to 15 mm/s, whereas gas circulation (regime 3) was achieved for velocities >60 mm/s. In general, the importance of regimes 1 and 2 decreases with scale. In large-scale reactors regime 1 is hardly realized and the transition from regime 2 to regime 3 depends strongly on sparger design and reactor geometry (Heijnen et al., 1997).

Gas Hold-Up

Figures 2 and 3 illustrate the effect of solid loading and particle size, respectively, on the gas hold-up of the three-phase airlift reactor used in this study. In these figures, the gas hold-up is referred to the solid free reactor volume

$$\left(\varepsilon_{G_L} = \frac{V_G}{V_L + V_G} \right).$$

All reported data are for situations in which the solid is completely suspended in the reactor. Unloaded reactor data are the average of three measurements; results of different measurements were reproducible within 5% uncertainty.

Figure 2 reports the overall gas hold-up (ε_{G_L}) as a function of the gas superficial velocity (u_G) for various loadings of basalt (Fig. 2a) and biofilm-coated particles (Fig. 2b). Gas hold-up decreases with increasing solid loading. The largest differences are observed in the range of gas superficial velocities from 15 to 55 mm/s (regime 2).

The observed dependence of gas hold-up on the solid hold-up is consistent with that experimentally found in a similar system by Koide et al. (1985), who reported that the gas hold-up decreases with increasing solid concentration for the case of glass beads ($\rho_S = 2500$ kg/m^3) and bronze spheres ($\rho_S = 8770$ kg/m^3). Also, in the case of solids of lower density, gas hold-up was found to decrease with increasing solid loading, as reported by Miyahara and Kawate
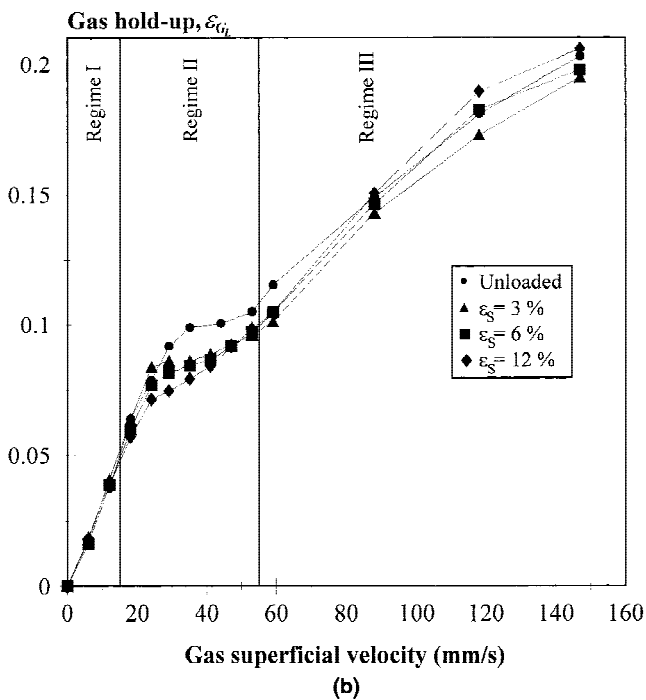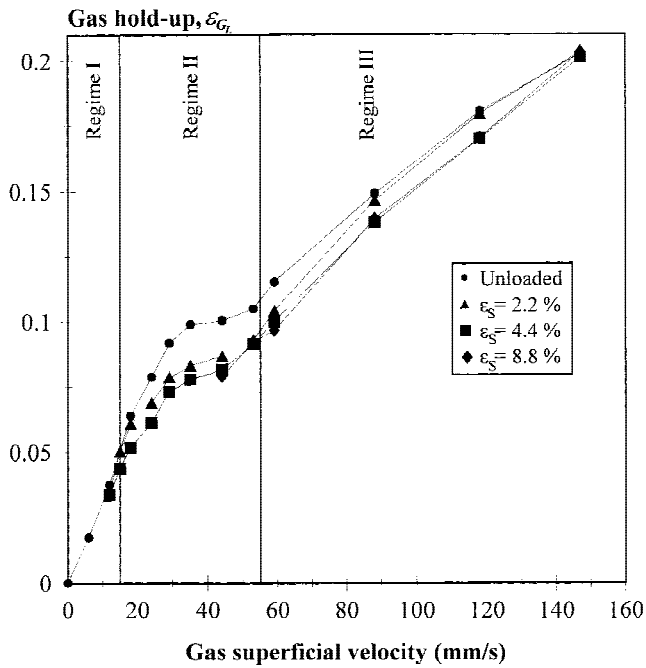
Figure 2. Effect of gas velocity on the gas hold-up for different solid loadings and constant particle size. (a) Basalt particles (d_S = 0.34 mm). (b) Biofilm-coated particles (d_S = 1.95 mm).

effect of solid concentration on gas hold-up of a draft-tube bubble column with a slurry of activated carbon (ρ_S = 1682 to 1933 kg/m^3).

The influence of particle size on gas hold-up (ε_{G_L}) is shown in Figure 3. Gas hold-up is plotted as a function of gas superficial velocity for four sieve fractions of basalt and for four sieve fractions of biofilm-coated particles in Figure 3a and b, respectively. Gas hold-up decreases with increas-
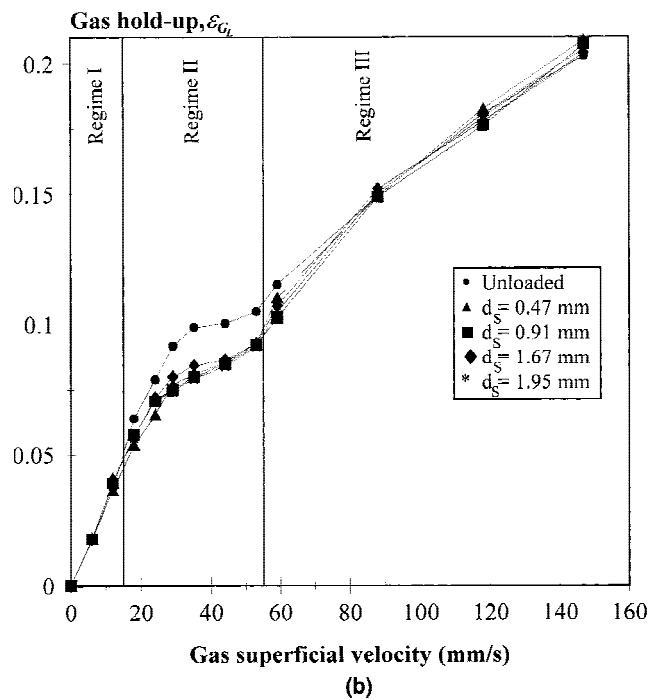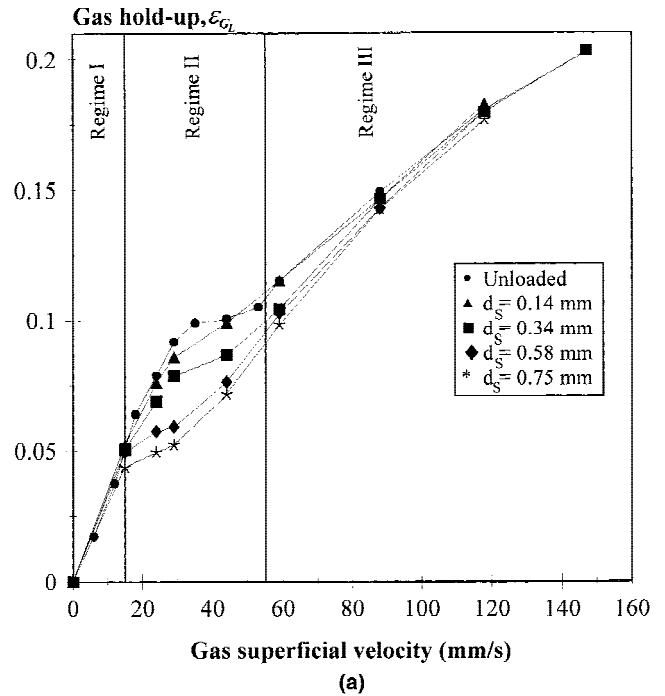
Figure 3. Effect of gas velocity on the gas hold-up for different solid size and constant solid loading. (a) Basalt particles (ε_S = 2.2%). (b) Biofilm-coated particles (ε_S = 12%).

(1993) for plastic beads (ρ_S = 1043 to 1135 kg/m^3), by Hwang and Lu (1997) for polystyrene cylinders (ρ_S = 1050 kg/m^3), and by Lu et al. (1995) for calcium-alginate beads (ρ_S = 1030 kg/m^3). The effect of solid is particularly noticeable at low gas velocity, as observed by Livingston and Zhang (1993), whose hydrodynamic model of a three-phase airlift reactor is consistent with the data of Koide et al. (1985). Only Muroyama et al. (1985) found a very slight

ing solid size in the case of basalt (Fig. 3a); the differences are again considerable in the range of gas superficial velocities from 15 to 55 m/s (regime 2). The influence of biofilm-coated particles is different. In this case (Fig. 3b), gas hold-up does not depend strongly on solid size.

The effect of solid size should be mainly related to the effect of particle terminal settling velocity (u_t). The particle terminal settling velocity has a direct influence on the difference in solid hold-up between the riser and the downcomer ($\Delta\varepsilon_s$). In turn, the difference, $\Delta\varepsilon_s$, strongly influences the hydrodynamics of the system; that is, if the solid hold-up in the riser is larger than in the downcomer, the presence of solids lowers the driving head of the system, and then lowers the liquid circulation rate and gas recirculation (i.e., the gas residence) time (Heijnen et al., 1997).

The terminal settling velocities of the particles used in this work, calculated by assuming sphere geometry, are reported in Table I. It should be noted that the terminal settling velocity of basalt particles varied over a wider range (19 to 129 mm/s) than that of biofilm-coated particles (30 to 49 mm/s). Consequently, the influence of particle size is more noticeable in the case of basalt (Fig. 3a) than in the case of biofilm-coated particles (Fig. 3b).

The observed influence of solid size on the hydrodynamics is consistent with that found by other investigators for similar systems. Koide et al. (1985) reported that the gas hold-up in their column decreases with increasing terminal velocity of the particles, and this behavior has also been predicted by the model of Livingston and Zhang (1993). From the results reported in Table I and Figure 3 it can be concluded that, in the present study also, the gas hold-up decreases with increasing particle settling velocity.

The curves for ε_{G_L} versus u_G for 0.34-mm basalt at $\varepsilon_S = 2.2\%$ and 1.95-mm biofilm at $\varepsilon_S = 12\%$ are compared in Figure 4. Notwithstanding the differences in solid loading, density, and size, the two curves are very close to each other. It should be observed that the solid concentration and the settling velocity are almost the same in both cases, so it can be concluded that the influence of solid loading on the hydrodynamics of airlift reactors is due to the weight of solids charged in the system and not to the volume.

Information on flow regimes can be inferred from Figures 2 and 3. It is evident in these figures that the slope of the graph of ε_G versus u_G changes drastically on two occasions; furthermore, even if the values of u_G corresponding to these points vary with both solid loading and particle size, the curves always present a platform for values of u_G ranging from 25 to 55 mm/s. For $u_G < 25$ mm/s and $u_G > 55$ mm/s, the gas hold-up increases with increasing gas superficial velocity, with the influence of u_G being much stronger in the first case. A similar behavior has already been reported by Gavroy et al. (1995) for a slurry draft-tube bubble column. The platform corresponds to the range of u_G where the strongest influence of solid loading and particle size on gas hold-up was observed. Moreover, this region seems to correspond to the transition between the hydrodynamic regime of no gas recirculation (regime 1, observed for $u_G < 15$
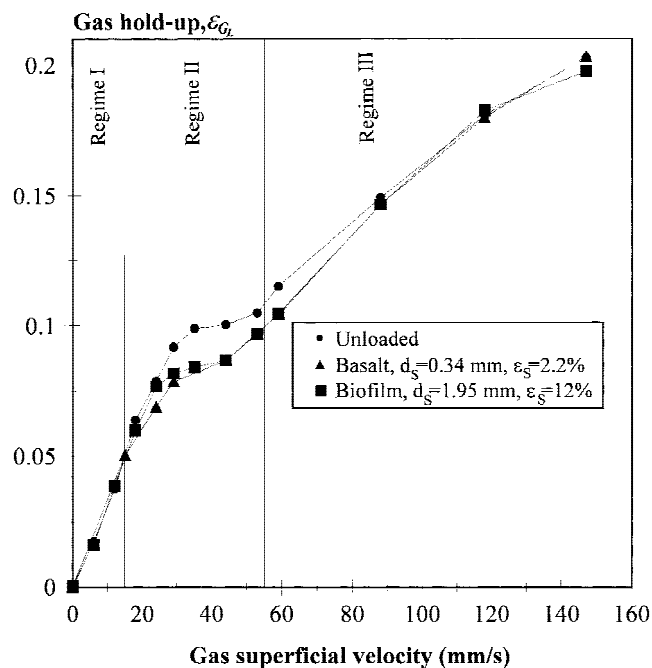
Figure 4. Gas hold-up as a function of gas velocity for basalt and biofilm-coated particles with similar settling velocity and particle concentration.

mm/s) and full gas recirculation (regime 3, observed for $u_G > 60$ mm/s); such transitions are indicated by the vertical lines in Figures 2 and 3.

Figure 5 compares the experimental gas hold-up (referred to in this case as the reactor volume), $\varepsilon_G = V_G/V_R$ measured for the unloaded reactor with the results reported by Bakker et al. (1993) for a 15-L internal-loop airlift reactor. Both sets of data show the same trend. Data on liquid circulation velocity reported by Bakker et al. (1993) are also plotted in Figure 5, where the vertical lines represent the regime tran-
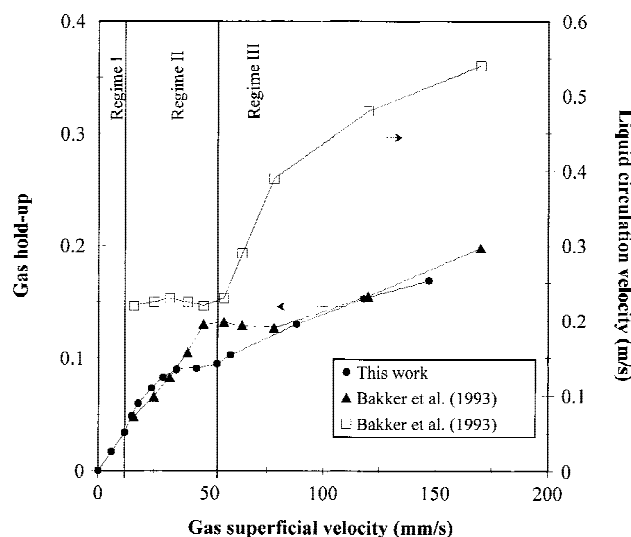
Figure 5. Gas hold-up and liquid circulation velocity in unloaded airlift reactors.

sitions observed in this work. The liquid circulation velocity changes drastically when the flow regime changes from 2 to 3, remaining almost constant in regime 2, and rapidly increasing with increasing gas velocity in regime 3.

Figure 6 compares the experimental gas hold-up, ε_G, measured for 0.34-mm basalt particles at $\varepsilon_S = 2.2\%$ with the values calculated according to the models proposed by Koide et al. (1985), Livingston and Zhang (1993), and Heijnen et al. (1997). The model of Heijnen et al. (1997) strongly overestimates the measured values, which, on the other hand, agree quite well with the estimates of Livingston and Zhang (1993) and Koide et al. (1985). The discrepancies are mainly due to the scale of the systems that the models represent. Livingston and Zhang (1993) and Koide et al. (1985) studied lab-scale reactors, whereas Heijnen et al. (1997) modeled the regime of complete gas recirculation, typical of larger scale reactors. Heijnen et al. (1997) reported that the gas recycling ratio is strongly scale-dependent; for small-scale columns, such as that used in this work as well as those used by Livingston and Zhang (1993) and Koide et al. (1985), the unrestricted carryover of gas bubbles into the downcomer is generally limited by frictional effects (wall friction, flow reversal at top and bottom, and losses due to the presence of the sparger). In lab-scale reactors, gas recirculation through the downcomer only occurs for gas superficial velocities much higher than in the cases of pilot- or full-scale reactors. As a consequence of the limited recirculation of gas (i.e., a limited volume of gas in the downcomer), laboratory reactors behave more as a bubble column than as a full-scale airlift reactor, as shown in Figure 6, where the gas hold-up calculated for a bubble column (according to the relationship proposed for the het-
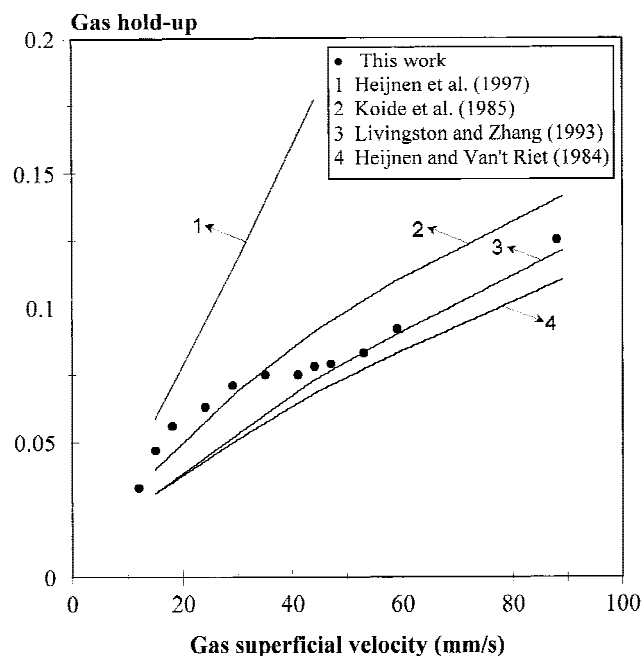
Figure 7. Comparison of experimental data and model predictions for volumetric mass transfer coefficient in airlift reactors and bubble columns.

erogeneous regime by Heijnen and Van 't Riet, 1984) compares well with the experimental estimates.

Volumetric Mass Transfer Coefficient

Figure 7 compares the volumetric mass transfer coefficient ($k_L a$) measured for the two-phase gas–liquid system with the correlation proposed by Heijnen and Van 't Riet (1984) for bubble columns. The $k_L a$ values measured in the present work are clearly higher than the values calculated for bubble columns. Gas–liquid mass transfer in bubble columns and airlift reactors is mainly determined by the diameter of the bubbles in the column. The bubble size, in turn, depends on many factors, mainly the coalescing property of the liquid, the type of sparger, and the scale of the column. The average bubble size can be calculated by:

$$d_b = \frac{6\varepsilon_G}{k_L a} k_L \tag{7}$$

Assuming a mass transfer coefficient, k_L, of 0.4 mm/s, the bubble sizes in the experiments of Figure 7 range from 3 to 4 mm. Similar values have been reported for porous plate spargers in water (Heijnen and Van 't Riet, 1984). In coalescing media, such as water, the coalescence of bubbles usually proceeds within a distance of 0.5 to 1 m from the sparger, where bubble size reaches a value of about 6 mm independently of the sparger (Heijnen and Van 't Riet, 1984). The correlation reported by Heijnen and Van 't Riet (1984) is rigorously valid for coarse bubble systems, where the bubble size is approximately 6 mm. The height of the draft tube used in this study was only 0.36 m, so that bubble coalescence might not have been complete. Moreover, the

Figure 6. Comparison of experimental data and model predictions for gas hold-up in airlift reactors and bubble columns.

sintered glass sparger allowed the formation of small bubbles. For fine bubble systems, $k_L a$ is high in comparison with coarse bubble systems for low u_G values, whereas, at higher u_G values, $k_L a$ levels off markedly (Heijnen and Van 't Riet, 1984). Similar behavior can be observed in Figure 7.

Due to the very small scale of the column used in this work a comparison with mass transfer in similar larger systems is hardly relevant. Most of the published data on mass transfer in bubble columns with and without draft tube report lower volumetric mass transfer coefficients than those estimated in the present work. This is probably the result of the porous sparger used in this work.

All results for volumetric oxygen mass transfer coefficients are given in Figures 8 and 9. $k_L a$ estimations were repeated three times for the unloaded reactor with an uncertainty of less than 5%. $k_L a$ was calculated taking into account the delay of the oxygen probe with a first-order model [Eq. (5)]. The values of $k_L a$ calculated not considering this delay were, in most cases, about 10% lower than those calculated with the first-order model for the probe response.

Figure 8 shows the dependence of the ratio between the actual volumetric mass transfer coefficient ($k_L a$) and the corresponding volumetric mass transfer coefficient in the unloaded reactor [$(k_L a)_0$] on the solid loading for gas superficial velocities ranging from 12 to 29 mm/s. Data regarding the 0.34-mm basalt particles and 1.95-mm biofilm-coated-particles are reported in Figure 8a and b. $k_L a$ decreases with increasing ε_S for cases of both basalt and biofilm-coated particles. A rather different behavior was reported by Ryhiner et al. (1988) for a three-phase biofilm-fluidized sand-bed reactor. In that case, $k_L a$ was found to decrease with increasing amounts of clean sand and to be almost independent of the sand fraction with biofilm-covered particles. However, a comparison between the two systems is not straightforward, because they present inherently different hydrodynamic behaviors: In three-phase fluidization, the solid concentration varies along the bed height, being highest at the point where gas is introduced, whereas, in normal operation of airlift columns, solids are more uniformly distributed.

Figure 9 shows the dependence of $k_L a/(k_L a)_0$ on particle size for gas superficial velocities ranging from 12 to 29 mm/s in the case of basalt (Fig. 9a) and biofilm-coated particles (Fig. 9b). The solid hold-up was 2.2% and 12% for basalt and biofilm-coated particles, respectively. The behavior of basalt and biofilm-coated particles is different. $k_L a$ decreases with increasing d_S (i.e., with decreasing number of particles) in the case of basalt, whereas, it is almost constant in the case of biofilm-coated particles. These results are in contrast to those reported by Nguyen-Tien et al. (1985), who found that $k_L a$ in three-phase fluidized beds of small glass spheres ($d_S < 1$ mm) was independent of particle size. For this reason, the correlation between $k_L a$, gas velocity, and solid hold-up proposed by Nguyen-Tien et al. (1985) for three-phase fluidized beds, and extended by Nigam and Schumpe (1987) to the case of bubble columns
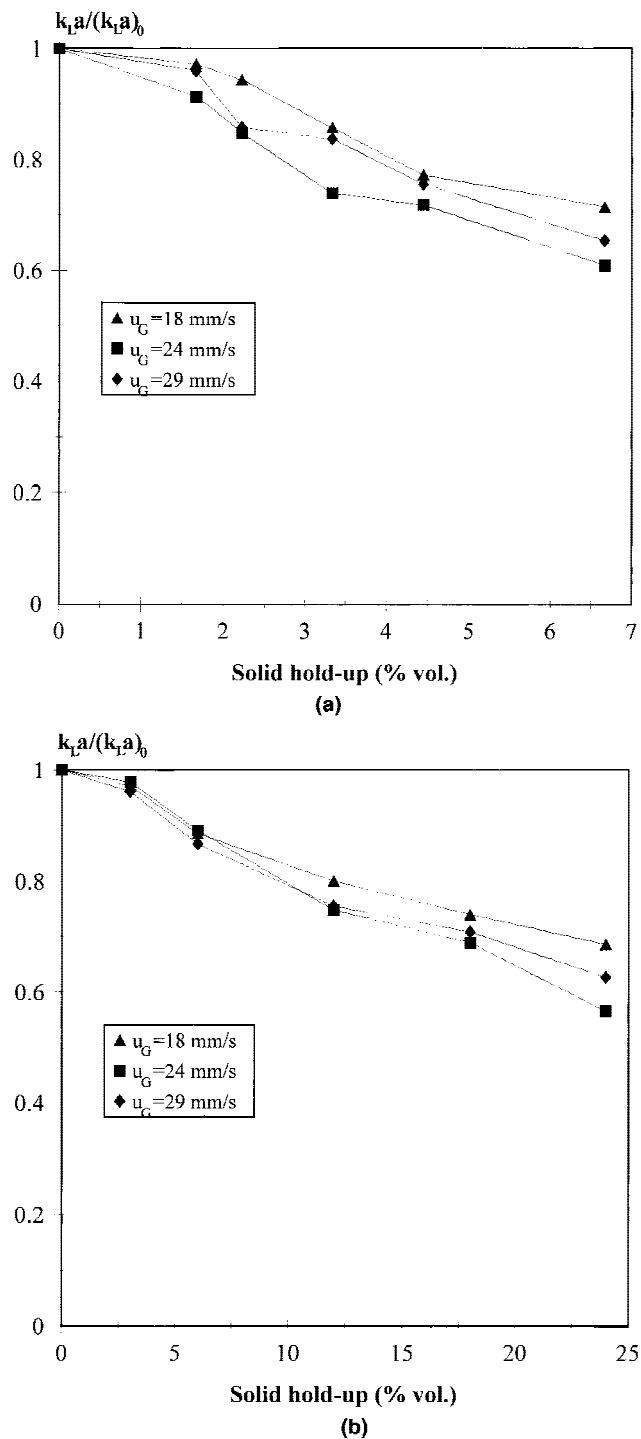
Figure 8. Effect of solid loading on volumetric mass transfer coefficient for different gas velocities and constant particle size. (a) Basalt particles ($d_S = 0.34$ mm). (b) Biofilm-coated particles ($d_S = 1.95$ mm).

with suspended solids, provides only a rough approximation (31% mean deviation) of the experimental results of this work. In this case, in addition to the different hydrodynamic characteristics of the systems considered, it should also be taken into account that the size of the reactors used by Nguyen-Tien et al. (1985) and Nigam and Schumpe (1987) were larger than that of the reactor used in this study; there-

(a)

(b)
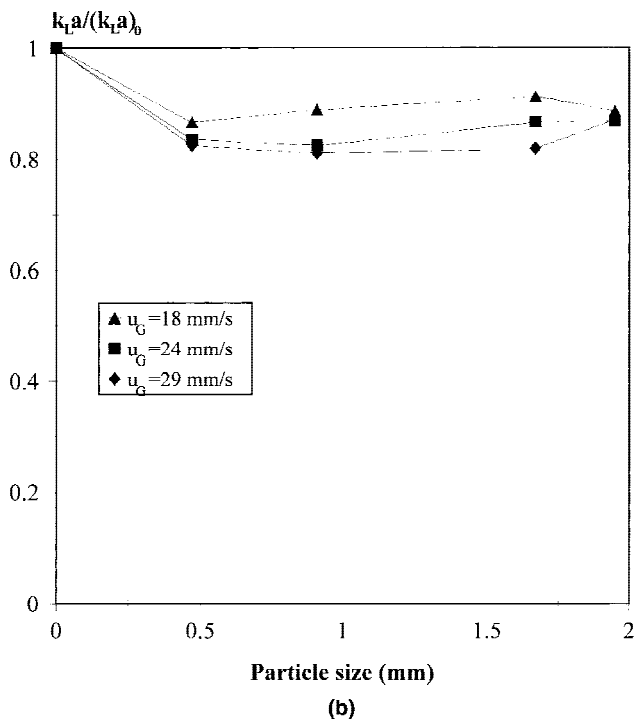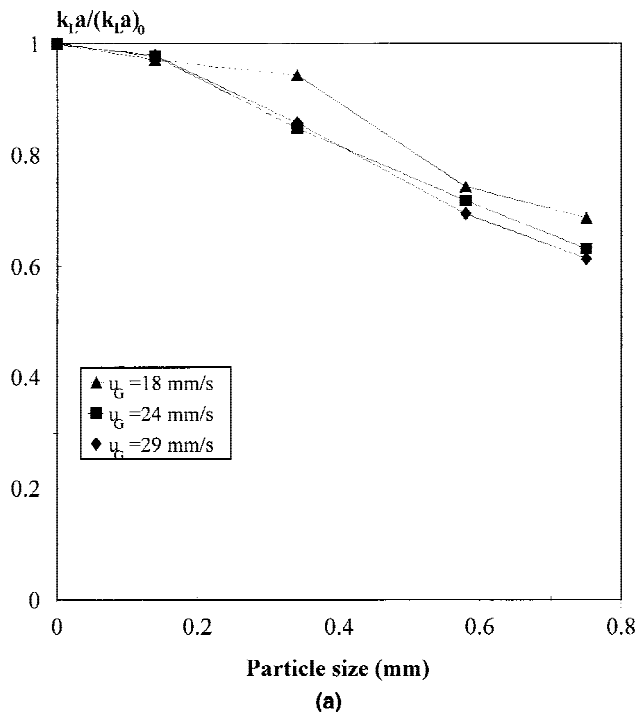
Figure 9. Effect of solid size on the volumetric mass transfer coefficient for different gas velocities and constant solid loading. (a) Basalt particles ($\varepsilon_S = 2.2\%$). (b) Biofilm-coated particles ($\varepsilon_S = 12\%$).

fore, as previously indicated, a comparison of the mass transfer characteristics is hardly relevant.

It appears from Figures 8 and 9 that, in the range examined, gas velocity does not considerably influence the effect of solid loading and particle size on k_La.

The volumetric mass transfer coefficient in airlift reactors is a strong function of gas hold-up; k_La is reported to be

proportional (McManamey and Wase, 1986) and even a low power (Koide et al., 1985) of ε_G. Figure 10 reports the values of k_La estimated in this work as a function of ε_G for the tests corresponding to different solid loadings and different solid sizes. The figure also shows a linear dependence between k_La and ε_G; this dependence is not influenced by solid loading, density, or size, so it may be concluded that the presence of solid affects only the gas hold-up (i.e., the total surface area of the gas bubbles) and not the mass transfer coefficient (k_L). The best linear description of the experimental data is:

$$k_La = [0.6 \text{ s}^{-1}]\varepsilon_G \qquad (8)$$

It can be inferred from Eq. (8) that the ratio between the mass transfer coefficient, k_L, and the bubble size, d_b, is a constant in the system studied in this work. This finding results explicitly after combining and rearranging Eqs. (7) and (8):

$$\frac{k_L}{d_b} = 0.1 \text{ s}^{-1}$$

Because k_L does not vary much with d_b (Heijnen and Van 't Riet, 1984), it may be concluded that bubble size is not influenced by the presence of solids in the system under study. Consequently, because the gas hold-up decreases with increasing solid hold-up, the presence of solids seems to lower the number of bubbles without changing their size.

CONCLUSIONS

Gas hold-up and volumetric mass transfer coefficient were measured in a lab-scale three-phase airlift reactor with an
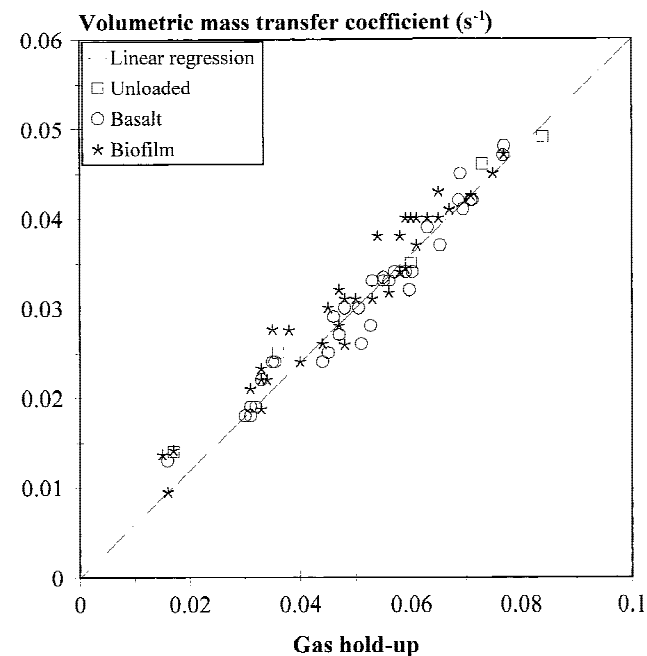
Figure 10. The volumetric mass transfer coefficient function of gas hold-up for different solid loading, density, and size.

internal draft tube. A previously derived relation between gas hold-up and gas velocity for large-scale (>100-L) airlift reactors proved to be invalid for application to small-scale (2-L) systems. These small systems behave as bubble columns under a heterogeneous flow regime.

The volumetric mass transfer coefficient was found to decrease with both solid hold-up and size. This was not due to modifications of mass transfer mechanisms, but rather to the effect that the presence of solids has on the gas hold-up, especially on the number of gas bubbles present in the system.

NOMENCLATURE

A_G	gas surface area (m^2)
A_B	biofilm surface area (m^2)
C^*	oxygen concentration at the gas–liquid interface (kg/m^3)
C_B	oxygen concentration in the biofilm (kg/m^3)
C_L	oxygen concentration in the liquid (kg/m^3)
C_P	oxygen probe response (kg/m^3)
d_b	bubble size (m)
d_C	clean support size (m)
d_S	solid size (m)
k_L	gas–liquid mass transfer coefficient (m/s)
$k_L a$	volumetric gas–liquid mass transfer coefficient (s^{-1})
$(k_L a)_0$	volumetric gas–liquid mass transfer coefficient at $M_S = 0$ (s^{-1})
k_P	probe constant (s^{-1})
k_S	liquid–solid mass transfer coefficient (m/s)
M_S	solid loading (kg)
t	time (s)
u_G	gas superficial velocity (m/s)
V_B	biofilm volume (m^3)
V_L	liquid volume (m^3)
V_R	reactor volume (m^3)

Greek letters

ε_G	gas hold-up (referred to reactor volume)
ε_{G_L}	gas hold-up (referred to liquid volume)
ε_S	solid hold-up

References

Bakker, W. A. M., van Can, H. J. L., Tramper, J., de Gooijer, C. D. 1993. Hydrodynamics and mixing in a multiple air-lift loop reactor. Biotechnol. Bioeng. **42**: 994–1001.

Beenackers, A. A. C. M., van Swaaij, W. P. M. 1993. Mass transfer in gas–liquid slurry reactors. Chem. Eng. Sci. **48**: 3109–3139.

Chisti, M. Y. 1989. Airlift bioreactors. Elsevier, London.

Chisti, M. Y., Moo-Young, M. 1987. Airlift reactors: Characteristics, applications and design considerations. Chem. Eng. Comm. **60**: 195–242.

Fuchs, R., Ryu, D. D. Y., Umphrey, A. E. 1971. Effect of surface aeration on scale-up procedures for fermentation processes. Ind. Eng. Chem. Proc. Des. Dev. **10**: 190–196.

Gavroy, D., Joly-Vuillemin, C., Cordier, G., Delmas, H. 1995. Gas hold-up, liquid circulation and gas–liquid mass transfer in slurry bubble-columns. Chem. Eng. Res. Des. (Part A) **73**: 637–642.

Gjaltema, A., Tijhuis, L., van Loosdrecht, M. C. M., Heijnen, J. J. 1995. Detachment of biomass from suspended non-growing spherical biofilms in airlift reactors. Biotechnol. Bioeng. **46**: 258–269.

Heijnen, J. J., Hols, J., van der Lans, R. G. J. M., van Leeuwen, H. L. J. M., Mulder, A., Weltevrede, R. 1997. A simple hydrodynamic model for the liquid circulation velocity in a full scale two and three phase internal airlift reactor operating in the gas recirculation regime. Chem. Eng. Sci. **52**: 2527–2540.

Heijnen, J. J., Mulder, A., Weltevrede, R., Hols, J., van Leeuwen, H. L. J. M. 1990. Large scale anaerobic/aerobic treatment of complex industrial waste water using immobilized biomass in fluidised bed and airlift suspension reactors. Chem. Eng. Technol. **13**: 145–220.

Heijnen, J. J., Van 't Riet, K. 1984. Mass transfer, mixing and heat transfer phenomena in low viscous bubble column reactors. Chem. Eng. J. **28**: B21–B42.

Hwang, S. J., Lu, W-J. 1997. Gas–liquid mass transfer in an internal loop airlift reactor with low density particles. Chem. Eng. Sci. **52**: 853–857.

Koide, K., Horibe, K., Kawabata, H., Ito, S. 1985. Gas holdup and volumetric liquid-phase mass transfer coefficient in solid-suspended bubble column with draught tube. J. Chem. Eng. Jpn. **18**: 248–254.

Livingston, A. G., Zhang, S. F. 1993. Hydrodynamic behaviour of three-phase (gas–liquid–solid) airlift reactors. Chem. Eng. Sci. **48**: 1641–1654.

Lu, W-J., Hwang, S. J., Chang, C-M. 1995. Liquid velocity and gas holdup in three-phase internal loop airlift reactors with low-density particles. Chem. Eng. Sci. **50**: 1301–1310.

McManamey, W. J., Wase, D. A. J. 1986. Relationship between the volumetric mass transfer coefficient and gas holdup in airlift fermentors. Biotechnol. Bioeng. **28**: 1446–1448.

Miyahara, T., Kawate, O. 1993. Hydrodynamics of a solid-suspended bubble column with a draught tube containing low-density particles. Chem. Eng. Sci. **48**: 127–133.

Muroyama, K., Mitani, Y., Yasunishi, A. 1985. Hydrodynamics characteristics and gas liquid mass transfer in a draft tube slurry reactor. Chem. Eng. Commun. **34**: 87–98.

Nguyen-Tien, K., Patwari, A. N., Schumpe, A., Deckwer, W-D. 1985. Gas–liquid mass transfer in fluidized particle beds. AIChE J. **31**: 194–201.

Nigam, K. D. P., Schumpe, A. 1987. Gas–liquid mass transfer in a bubble column with suspended solids. AIChE J. **33**: 328–330.

Perry, R. H., Green, D. 1984. Chemical engineers' handbook. 6th edition. McGraw-Hill, New York.

Reichert, P. 1994. Concepts underlying a computer program for the identification and simulation of aquatic system. Schriftenreihe der EAWAG No. 7. EAWAG, Switzerland.

Ryhiner, G., Petrozzi, S., Dunn, I. J. 1988. Operation of a three-phase biofilm fluidized sand bed reactor for aerobic wastewater treatment. Biotechnol. Bioeng. **32**: 677–688.

Sanger, P., Deckwer, W-D. 1981. Liquid–solid mass transfer in aerated suspensions. Chem. Eng. J. **22**: 179–186.